Modeling West Nile virus transmission in birds and humans: Advantages of using a cellular automata approach

Baki Cissé, David R Lapen, Karine Chalvet-Monfray, Nicholas H Ogden, Antoinette Ludwig

Modeling West Nile Virus transmission in birds and humans: Advantages of using a cellular automata approach

Baki Cissé [a, b, *], David R. Lapen [c], K. Chalvet-Monfray [d, e], Nicholas H. Ogden [a, b], Antoinette Ludwig [a, b]

[a] Public Health Sciences Division, National Microbiology Laboratory, Public Health Agency of Canada, St-Hyacinthe, Canada
[b] Groupe de Recherche en Épidémiologie des Zoonoses et Santé Publique (GREZOSP), Faculté de Médecine Vétérinaire, Université de Montréal, Saint-Hyacinthe, Québec, Canada
[c] Ottawa Research and Development Centre, Science and Technology Branch, Agriculture and Agri-Food Canada, Ottawa, K1A 0C6, Canada
[d] Université de Lyon, INRAE, VetAgro Sup, UMR EPIA, Marcy l'Etoile, France
[e] Université Clermont Auvergne, INRAE, VetAgro Sup, UMR EPIA, Saint-Genès-Champanelle, France

ARTICLE INFO

ABSTRACT

In Canada, the periodic circulation of West Nile Virus (WNV) is difficult to predict and, beyond climatic factors, appears to be related to the migratory movements of infected birds from the southern United States. This hypothesis has not yet been explored in a spatially distributed model. The main objective of this work was to develop a spatially explicit dynamic model for the transmission of WNV in Canada, that allows us to explore non-climate related hypotheses associated with WNV transmission. A Cellular Automata (CA) approach for multiple hosts (birds and humans) is used for a test region in eastern Ontario, Canada. The tool is designed to explore the role of host and vector spatial heterogeneity, host migration, and vector feeding preferences.

We developed a spatialized compartmental SEIRDS-SEI model for WNV transmission with a study region divided into 4 km^2 rectangular cells. We used 2010—2021 bird data from the eBird project and 2010—2019 mosquito data collected by Ontario Public Health to mimic bird and mosquito seasonal variation. We considered heterogeneous bird densities (high and low suitability areas) and homogeneous mosquito and human densities. In high suitability areas for birds, we identified 5 entry points for WNV-infected birds. We compared our simulations with pools of WNV-infected field collected mosquitoes. Simulations and sensitivity analyses were performed using MATLAB software.

The results showed good correspondence between simulated and observed epidemics, supporting the validity of our model assumptions and calibration. Sensitivity analysis showed that a 5% increase or decrease in each parameter of our model except for the biting rate of bird by mosquito ($c^{(B,M)}$) and mosquito natural mortality rate (d^M), had a very limited effect on the total number of cases (newly infected birds and humans), prevalence peak, or date of occurrence. We demonstrate the utility of the CA approach for studying WNV transmission in a heterogeneous landscape with multiple hosts.

* Corresponding author. Public Health Sciences Division, National Microbiology Laboratory, Public Health Agency of Canada, 3200 Sicotte, St Hyacinthe (QC) J2S 2M2, Canada.
E-mail addresses: baki.cisse@phac-aspc.gc.ca (B. Cissé), antoinette.ludwig@phac-aspc.gc.ca (A. Ludwig).

1. Introduction

According to World Health Organisation Vector-Borne Diseases (VBDs) are a major threat to the health of populations around the world and are responsible for more than 17% of all infectious diseases and at least 700 000 deaths annually. VBDs also weigh heavily on economies and limit rural and urban development (WHO, 2017). Historically less problematic in Canada, VBDs have become a significant public health threat in recent years (Mathieu & Karmali, 2016).From 1994 to 2008, they were responsible for 24 028 encephalitis-associated hospitalizations in Canada (Kulkarni et al., 2013)

The mosquito-borne West Nile Virus (WNV) is a zoonotic pathogen that belongs to the Flaviviridae family (Vogels et al., 2017). First described in Uganda in 1937, WNV appeared in North America in New York State in September 1999 and spread to Canada in 2001 (Abdelrazec et al., 2014; Ludwig et al., 2010; Mallya et al., 2018). WNV is recognized as the most important mosquito-borne disease in Canada (Ludwig et al., 2019; PHAC, 2021). Therefore, it has attracted a great deal of interest from researchers and public authorities who have undertaken many studies to better understand and control it (Moua et al., 2021; PHAC, 2021; Ripoche et al., 2019). In ~70% of cases, infections in humans are asymptomatic, but some experience symptoms such as fever, headache, a skin rash, and muscle aches. In a few cases, particularly patients older than 50, the infection can lead to more severe neuroinvasive disease (meningitis or encephalitis) resulting in death in approximately 10% of these cases (Badawi et al., 2018; Fasano et al., 2022; Ouhoumanne et al., 2018).

In eastern Canada, WNV is thought to be principally transmitted by the mosquitoes *Culex pipiens* and *Culex restuans* — identified as *Culex pipiens-restuans* (*Cx. Pipiens-restuans* (CPR)) to birds, humans, and horses (Moua et al., 2021).

Several studies have identified the CPR mosquitoes as the main vector responsible for WNV cases, and the American Robin (*Turdus migratorius*) is suspected to be the main amplifying host or reservoir of WNV in Canada (Kilpatrick et al., 2006; Taieb et al., 2020). Humans and horses are considered primarily as dead-end hosts (Moua et al., 2021; Taieb et al., 2020). Since 2003, all suspected or confirmed cases of WNV in livestock must be reported to the Canadian Food Inspection Agency (CFIA). WNV in humans is a nationally notifiable disease, and cases detected are reported to the Public Health Agency of Canada (PHAC), by provincial or territorial public health organizations. As WNV can be transmitted in blood products, Canadian Blood Services and Héma-Québec also participate in human case surveillance by testing Canadian blood donors for WNV (TodoricD et al., 2022; 48(5):181–7.). The prevalence of the disease is generally low in Canada. In 2021, from January to October, 29 clinical human cases and five asymptomatic human cases of WNV were reported to the PHAC (PHAC, 2021). However, in some years more serious outbreaks occur (particularly in 2007 in the Prairie provinces, and 2012 and 2018 in Ontario and Quebec (Canada)), likely driven by effects of weather on mosquito populations and WNV transmission cycles.

There is extensive literature on mathematical modeling of WNV, with a range of objectives such as understanding the role of birds (corvids and non-corvids) (Abdelrazec et al., 2014), the impact of seasonal variation in the mosquito population (Wonham et al., 2004), the temporal transmission of the virus in the mosquito-bird cycle (Cruz-Pacheco et al., 2005), or the effect of mosquito reduction strategies and human exposure to mosquito bites (Bowman et al., 2005).

Most studies use approaches that do not consider spatial aspects of transmission and virus spread (Abdelrazec et al., 2014; Bowman et al., 2005; Cruz-Pacheco et al., 2005; Wonham et al., 2004). Spatial modeling of West Nile is an underutilized but important aspect of understanding the dynamics of this disease. The transmission of WNV in Canada, and the evolution of outbreaks, are highly dependent on seasonal variations and are often localized geographically (TodoricD et al., 2022; 48(5):181–7.). The hypotheses related to the seasonality of cases (late August–September) are fairly well established and related to both changes in mosquito feeding preferences (Kilpatrick et al., 2006; Taieb et al., 2020) and decreasing host abundance (caused by migration, among other things). The reasons for spatial segregation of cases are less well established; however, it is thought to be related to human abundance, spatial heterogeneity of host (bird) and vector (mosquito) abundances but also to migratory movements (in spring and autumn) of birds (Talbot et al., 2019). A cellular automata (CA) approach to spatial modeling may allow us to explore many of these driving factors via a single modeling tool (Lin & Zhu, 2017; Zhang et al., 2018).

CA can be conceptualized as a discrete mathematical model in which the n-dimensional Euclidean space is subdivided into regular cells that, at a particular point in time, can have only one of a finite number of states. These states are updated at discrete time steps, considering the states of neighbouring cells (B. Cissé, El Yacoubi, & Gourbière, 2016a, 2016b; Slimi et al., 2009). CA models can describe the complexity of real world spatially extended systems by way of local transition rules that may be expressed as algorithms and then easily implemented as computer programs. They are a powerful tool for modeling biological systems in general, and spatial epidemiology in particular (B. Cissé et al., 2016a, 2016b; Mikler et al., 2005; Ruhomally et al., 2022; Sirakoulis et al., 2000). CA models have been successfully used to study several VBDs (B. Cissé et al., 2016a, 2016b; Baki Cissé et al., 2016a, 2016b; Cissé, El Yacoubi, & Tridane, 2013; Cissé et al., 2014; Doran & Laffan, 2005; White et al., 2007) around the world, and the approach is an interesting opportunity for modeling WNV transmission.

In this study, we present the development of a CA approach to simulate the spread of WNV in eastern Ontario, Canada in the case of multiple hosts (birds and humans). The tool is designed to explore the role of host spatial heterogeneity and migration, as well a vector spatial heterogeneity and feeding preferences, on the local transmission and amplification of WNV.

Specifically here we explore the transmission of WNV in southeastern Canada under the assumption that WNV is introduced each year via infection of birds migrating north from the US as suggested by phylogeographic analyses (Reisen & Wheeler, 2019; Therrien et al., 2019). An alternative hypothesis of annual infection of breeding birds by overwintering infected mosquitoes (Andreadis, 2012; Reisen & Wheeler, 2019) will be explored in the future.

2. Materials and methods

2.1. Cellular automata overview

First described by Von Neumann in the early 1950s to serve as a simple model of self-reproduction in biological systems (Neumann, 1966), CA are now broadly used to model complex systems in several fields such as computer science, mathematics, engineering, biology and epidemiology (Mange & Tomassini, 1998; Margolus, 1984; Ruhomally et al., 2022; Sipper, 1994; Vichniac, 1984; Wang et al., 2023) [28, 38−42].

A cellular automaton is generally defined as a regular lattice of cells, each having an identical pattern of local connections with other cells and being subject to given boundary conditions. Each cell can take a state, among a finite set of states, which are updated at every time step according to local transition rules describing the transmission dynamics of the endpoint of interest. Time progresses in discrete steps. The state of a cell at time $t + 1$ is a function of its own state and of the states of its neighbours at time t (B. Cissé et al., 2016a, 2016b).

The mathematical formalism of CA is presented as follows (from (B. Cissé et al., 2016a, 2016b)):

Definition: A CA is defined by a quadruple $A = (\mathscr{L}, S, N, f)$ where:

- $\mathscr{L}$ is a d-dimensional lattice of cells c that are arranged according to the dimension of the space and the shape of the cells.
- S denotes a set of discrete states. It is a discrete finite set often represented by numbers. It is defined as the set of possible values that can take any state of the cell. It is generally a cyclic ring of dimension k noted $S = \{s_1, s_2, ..., s_k\}$
- N is a mapping that defines the cell's neighborhood. It is the set of cells $c_i, i \in \{1, 2, ..., n\}$ which interact with cell c at time t to influence its state at time $t + 1$. It's noted

$$N : \mathscr{L} \to \mathscr{L}^n$$

$$c \to N(c) = (c_1, c_2, ..., c_n)$$
where n is the size of the neighborhood.

- f is a transition function which allows to calculate the cell's state at time $t + 1$ given the neighborhood's state at time t. It can be defined by:

$$f : S^n \to S$$

$$s_t(N(c)) \to s_{t+1}(c) = f(s_t(N(c)))$$

where $s_t(c)$ designates the state of the cell c at time t and $s_t(N(c)) = \{s_t(c^{\cdot}), c^{\cdot} \in N(c)\}$ is the neighborhood state.

The CA state or configuration at time t is the set $\{s_t(c), c \in \mathscr{L}\}$ given by:

$$s_t : \mathscr{L} \to S$$

$$c \to s_t(c)$$

2.2. Model assumptions

Our model analyzes the interactions between three groups of individuals: birds, mosquitoes and humans. All individuals are identified by their clinical status. Each individual, depending on the group they belong to, is regrouped by states. The possible states are: Susceptible, Exposed, Infectious, Recovered or Dead. However, each group doesn't contain all states. Susceptible are those who are susceptible to infection with the disease, Exposed individuals are infected but not infectious (cannot yet transmit the disease), Infectious individuals are those who can transmit the disease to susceptible vectors, and

Recovered individuals are those who are immune or cured with the possibility of becoming susceptible again. Those who have died of the disease are called Dead individuals. Our model is based on the following additional assumptions:

- Birds and humans, at each stage of their lives, can become Susceptible, Exposed, Infectious, Recovered or Dead. These subclasses have been used successfully in several disease modeling efforts (Bowman et al., 2005; Shaman, 2007). Birds are the only competent host (Taieb et al., 2020); that is, they can transmit the disease to mosquito. Although humans can get to the 'Infectious' status in our model, they are considered as incompetent host (Bowman et al., 2005) which here means that the level of infectiousness is not high enough to infect a mosquito. They can, however, be infectious by direct transmission in very specific cases like during blood transfusion, organ transplant or mother to baby during pregnancy, delivery or breast feeding (CDC, 2021).
- Mosquitoes, considered as principally represented by *Culex pipiens-restuans* (CPR), have a short lifespan and can only become Susceptible, Exposed or Infectious (Durand et al., 2010; Ewing et al., 2021; Wonham et al., 2004).
- The CA cell size ($2 \times 2\ km^2$) represent an average home range size for the American Robin, which is identified as the most viable reservoir species in Canada (Kilpatrick et al., 2006; Taieb et al., 2020). In Massachusetts, robin home range averaged about 400 m radius around nests (Hirth et al., 1969) and in Wisconsin, it ranged from 445 *to* 2420 m^2, with an average of 1210 m^2 (Young, 1950).
- Only birds can move between cells. In a time step, these movements are only made by a proportion of birds, which are mainly adults during the breeding season and a mix of juveniles and adults later, until fall migration.
- Humans are assumed to stay within their own cells. This assumption is introduced for the sake of simplicity. Indeed, as man is an accidental host, we have decided to focus solely on the movements of the main host (birds) to reduce the complexity of the equations and make the analysis of the model simpler and clearer. However, movements of humans (incidental hosts) between cells, related to their work, their habitats, their leisure, etc … could be explored in future work, as the model will allow such parameterization.
- Mosquitoes also do not move outside their own cells, as CPR mosquitoes mostly spend their entire life within a few square kilometers (Ciota et al., 2012; Moua et al., 2021).

2.3. Delimitation of seasonality

Because of its importance, seasonality in epidemic models has been the subject of several studies (Buonomo et al., 2018).

In our study, we assumed that mosquito and bird abundances vary over the year according to the cyclical regular variations inherent to the species biology. Each year was divided into four parts based on robin and CPR behavior (Fig. 1). The first one represents the cold season (blue solid line in Fig. 1) that begins on October 1 (day 274) and ends on March 31 (day 90) (Robert et al., 2019). During the cold season, the number of birds decreases due to natural mortality. At the very early stage of the cold season, we assume that there are still mosquitoes present in our cells until day 303 (October 30), which is confirmed by the observational data of mosquito surveillance held by Public Health Ontario (PHO) for the study region (PHO, 2021).

The second season, called the spring bird migration and breeding season (green dotted line in Fig. 1), begins on April 1 (day 91) and ends on July 31 (day 212) (Robert et al., 2019). During this spring season, birds arrive in our study area. These movements represent the massive seasonal migration of birds that occur in large areas of Canada, United States, and Mexico, each spring (Oliver et al., 2020; Rappole et al., 2000; Taieb et al., 2020; Vanderhoff et al., 2016). Considering the location of our study region, the migratory flyways used by the birds is the Atlantic flyway, stretching from Florida to Greenland, this flyway contains all of North America's Atlantic coast and the Appalachian chain (Belkhiria et al., 2016). From April 15 (day 105), the birds begin to breed and raise their young. The brood size and duration correspond to the ones observed for the American robin (Robert et al., 2019; Vanderhoff et al., 2016). Only a certain percentage of migratory birds can be infected when arriving in our study region and it can happen only between May 1 (day 121) to June 30 (day 181) (Robert et al., 2019). This time is designated as the infected bird arrival period (green solid line) in our model. It was chosen to coincide with the resumption of vector mosquito activity in late spring. Infected birds arrive in specific cells selected on the fact that they had the highest average bird robin density according to eBird observation data (Cornell Lab of Ornithology, Oct 2021).

The third season is named the summer season (red solid line) and corresponds to post breeding and dispersal of the young birds born in the summer. It covers the whole month of August (day 213 - day 243) (Robert et al., 2019). During these first flights, young usually travel less than half a mile (about 0.8 km) to find food (Hirth et al., 1969) while remaining under the supervision of their parents (Weatherhead & McRae, 1990).
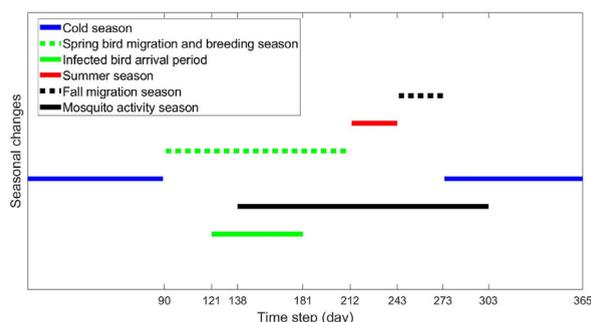
Fig. 1. Seasonal changes in bird behavior and mosquito activity.

The last bird season is named the fall migration season (black dotted line), which occurs in September (from day 244 to day 273 (Robert et al., 2019)); corresponding to when robin (adults and juveniles) can leave the study region to migrate south (Robert et al., 2019; Vanderhoff et al., 2016). We considered that around half of the robin population migrate southern for winter and this group of migratory birds consists of both adults and juvenile birds of the year.

The mosquito season is referred to as the mosquito activity season (black solid line) and is based on observational data from PHO mosquito surveillance (PHO, 2021). It begins on CDC week 21 (day 138 corresponding to May 18) and ends on CDC week 42 (day 303 corresponding to October 30). It covers the entire summer season and partially overlaps the spring bird migration and breeding season and cold season.

Finally, the human population is considered spatially and temporally stable throughout the year, except for natural mortality which slightly decreases the abundance of humans. We also didn't consider any specific behavioral variation that could lead to associated variation in risk of exposure from mosquito bites.

2.4. CA approach

We propose a compartmental cellular automata model with a competent host (bird (Taieb et al., 2020)) denoted B, an incompetent host (human (Bowman et al., 2005)) denoted H and a vector (mosquito) denoted M. This is a SEIRDS-SEI model defined as follows:

- The space $\mathscr{L}$, represented by a two-dimensional square lattice where a cell is given by its coordinates (i,j) and can be occupied by hosts or/and vectors. Each cell represents a square lattice 4 km^2.
- The state $s_t(i,j)$ of each cell (i,j) at the time t is given by the triplet

$$s_t(i,j) = \left(s_t^B(i,j), s_t^H(i,j), s_t^M(i,j) \right)$$

where $s_t^B(i,j)$, $s_t^H(i,j)$, $s_t^M(i,j)$ the state of bird, human and mosquito at time t. They are presented as follow:

- $s_t^B(i,j) = (S_t^B(i,j), E_t^B(i,j), I_t^B(i,j), R_t^B(i,j), D_t^B(i,j))$ gives the number of susceptible, exposed, infectious, recovered or dead birds in cell (i,j) at time t,
- $s_t^H(i,j) = (S_t^H(i,j), E_t^H(i,j), I_t^H(i,j), R_t^H(i,j), D_t^H(i,j))$ gives the number of susceptible, exposed, infectious, recovered or dead humans in cell (i,j) at time t,
- $s_t^M(i,j) = (S_t^M(i,j), E_t^M(i,j), I_t^M(i,j))$ gives the number of susceptible, exposed and infectious vectors in cell (i,j) at time t.
- The neighborhood N_{ij} of cell (i,j) of size n, given by the set $\{(i+\alpha_1, j+\beta_1), (i+\alpha_2, j+\beta_2), ..., (i+\alpha_n, j+\beta_n)\}$ where $\{(\alpha_k, \beta_k)\ 1 \leq k \leq n\} \in Z \times Z$. In our study, we use Moore neighborhood (Kari, 2005) in which

$$(\alpha_k, \beta_k)_{1 \leq k \leq 8} \in N^* = \{(1,0), (1,1), (0,1), (-1,1), (-1,1), (0,-1), (-1,-1), (1,-1)\}$$

The Moore neighborhood has been used successfully in several epidemiological models (Cissé et al., 2014; Sirakoulis et al., 2000; White et al., 2007).

- The transition function f, a local transition rule which updates the state of each cell (i,j) at time $(t+1)$ in terms of the states of its neighbouring cells at time t. The changes in $s_t^B(i,j)$, $s_t^H(i,j)$ and $s_t^M(i,j)$ are computed according to the dynamics of the disease transmission.

The demographic dynamics of the hosts and vectors are integrated in our model by recruitment and mortality rates. The model also considers the impact of the distance between a central cell and its neighbouring cells through the parameter $d^{(\alpha_k, \beta_k)}(i,j)$.

With

$$d^{(\alpha_k, \beta_k)}(i,j) = \frac{\frac{1}{\|(i,j)-(i+\alpha_k, j+\beta_k)\|_2}}{\sum_{(\alpha_k, \beta_k) \in N^*} \frac{1}{\|(i,j)-(i+\alpha_k, j+\beta_k)\|_2}} = \frac{\frac{1}{\sqrt{\alpha_k^2 + \beta_k^2}}}{\sum_{(\alpha_k, \beta_k) \in N^*} \frac{1}{\sqrt{\alpha_k^2 + \beta_k^2}}}$$

where $\|.\|_2$ represent the Euclidian norm. It is a weight coefficient associated to the number of susceptible birds in the neighbouring cell $(i+\alpha_k, j+\beta_k)\ 1 \leq k \leq 8$, moving to the cell (i,j) with a probability $\mu_B(i,j)$.

The transmission of the pathogen can occur in two different ways. The first one is by contact between infectious mosquitoes and susceptible birds with the parameter β_{BM} or human with the parameter β_{HM}. The second way to transmit the disease is by contact between an infectious bird and a susceptible mosquito with transmission rate β_{MB}. We assume that humans and mosquitoes can only be infected in their own cells, as they cannot move through the network.

The conceptual diagram that shows all the interactions between our three types of agents is shown in Fig. 2.

The epidemiological dynamics under the above assumptions is governed by equations (1)–(5) for birds.
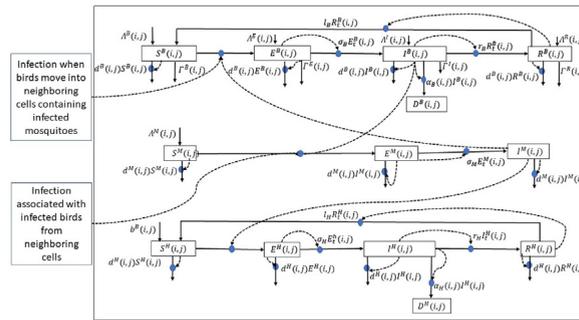
Fig. 2. Conceptual diagram of the West Nile Virus transmission model within one cell of the Cellular Automata grid in bird (B), mosquito (M) and human (H) populations. Boxes indicate states in each population and arrows between boxes indicate rates of flow between states. The possible states are: Susceptible, Exposed, Infectious, Recovered or Dead. Dashed arrows indicate parameters that influence the transition from one compartment to another. Notations and parameters are explained in Table 1. The conceptual diagram also represents the connexion with birds and mosquito populations in neighbouring cells and their influence (dashed arrow) on transition between susceptible state and exposed states of birds and mosquito populations of the cell.

Table 1
Parameters of the WNV model.

Definition	Symbol	Dimension	Estimate	Sources
Vector demography and feeding				
Mosquito recruitment flow	Λ^M	day^{-1}	—	PHO (2021)
Mosquito natural mortality rate	d^M	day^{-1}	0.096	Jones et al. (2012)
Rate of biting of bird by mosquito	$c^{(B,M)} = c^{(M,B)}$	day^{-1}	0.11 (See Appendix A.1)	(Khalil et al., 2021; Wonham et al., 2004)
Rate of biting of human by mosquito	$c^{(H,M)} = c^{(M,H)}$	day^{-1}	0.192 (See Appendix A.2)	(Brugman et al., 2017; Ryan et al., 2017)
Rate of Mosquitoes that feed on the bird	p^B	—	]0, 1] (See Appendix A.3)	
Rate of Mosquitoes that feed on the human	p^H	—	]0, 1] (See Appendix A.3)	
Host demography				
Bird recruitment flow	Λ^B	day^{-1}	—	(Cornell Lab of Ornithology, Oct 2021)
Bird departure flow	Γ	day^{-1}	—	
Bird dispersal rate	μ_B	—	[0.4, 1]	
Time spent in the origin cell by moving birds	τ	—	0.4	[a]
Bird natural mortality rate	d^B	day^{-1}	0.00055	Farner (1949)
Human birth rate	b^H	day^{-1}	0.00003 (See Appendix A.4.)	StatCan (2022a)
Distance impact factor	$d^{(\alpha_k,\beta_k)}$	—	$\left\{\dfrac{1}{4+2\sqrt{2}}, \dfrac{1}{\sqrt{2}(4+2\sqrt{2})}\right\}$	White et al. (2007)
Human natural death rate	d^H	day^{-1}	0.00003 (See Appendix A.5.)	StatCan (2022b)
Pathogen transmission				
Per contact probability of transmission from Mosquito to bird	β_{BM}	—	1	Komar et al. (2003)
Per contact probability of transmission from bird to mosquito	β_{MB}	—	0.36	Komar et al. (2003)
Per contact probability of transmission from mosquito to human	β_{HM}	—	1	Komar et al. (2003)
Pathogen within-host dynamics				
Pathogen virulence to infectious bird	α_B	day^{-1}	0.066	VanDalen et al. (2013)
Pathogen virulence to infectious human	α_H	day^{-1}	0.0009 (See Appendix A.6.)	(PHAC, 2010, 2015)
Recovery rate for bird	r_B	day^{-1}	0.25	VanDalen et al. (2013)
Recovery rate for human	r_H	day^{-1}	0.22 (See Appendix A.7.)	PHAC (2010)
Incubation period for bird	$1/\sigma_B$	day	1	VanDalen et al. (2013)
Incubation period for human	$1/\sigma_H$	day	8.5 (See Appendix A.8.)	PHAC (2015)
Incubation period for mosquitoes	$1/\sigma_M$	day	4	Dohm et al. (2002)
Rate of the loss of immunity for bird	l_B	day^{-1}	0.00055	[b]
Rate of the loss of immunity for human	l_H	day^{-1}	0.00055	[b]

[a] τ is a part of the time step i.e. $\tau < t$

[b] There is considerable uncertainty regarding the protective immunity against West Nile virus. Considering protective immunity observed in small birds (Nemeth et al., 2009), we assumed that both infected birds and human will have a protective immunity of 5 years. Therefore, the rate of loss of immunity is estimated to be $1/(5 \times 365) \approx 0.00055$. https://www.cdc.gov/westnile/index.html.

$$S_{t+1}^B(i,j) = S_t^B(i,j) + \Lambda_t^B(i,j) - d_t^B(i,j)S_t^B(i,j) - \Gamma_t^B(i,j) + l_B R_t^B(i,j)$$

$$-(1 - \mu_B(i,j))c_t^{(B,M)}(i,j)p_t^B(i,j)\beta_{BM}\frac{S_t^B(i,j)I_t^M(i,j)}{N_t^B(i,j)}$$

$$-\mu_B(i,j)\tau c_t^{(B,M)}(i,j)p_t^B(i,j)\beta_{BM}\sum_{(\alpha_k,\beta_k)\in N^*}d^{(\alpha_k,\beta_k)}(i,j)\frac{S_t^B(i,j)I_t^M(i+\alpha_k,j+\beta_k)}{N_t^B(i,j)}$$

$$-\mu_B(i,j)(1-\tau)c_t^{(B,M)}(i,j)p_t^B(i,j)\beta_{BM}\frac{S_t^B(i,j)I_t^M(i,j)}{N_t^B(i,j)} \tag{1}$$

$$E_{t+1}^B(i,j) = E_t^B(i,j) + \Lambda_t^E(i,j) - d_t^B(i,j)E_t^B(i,j) - \Gamma_t^E(i,j) - \sigma_B E_t^B(i,j)$$

$$+(1 - \mu_B(i,j))c_t^{(B,M)}(i,j)p_t^B(i,j)\beta_{BM}\frac{S_t^B(i,j)I_t^M(i,j)}{N_t^B(i,j)}$$

$$+(i,j)\tau c_t^{(B,M)}(i,j)p_t^B(i,j)\beta_{BM}\sum_{(\alpha_k,\beta_k)\in N^*}d^{(\alpha_k,\beta_k)}(i,j)\frac{S_t^B(i,j)I_t^M(i+\alpha_k,j+\beta_k)}{N_t^B(i,j)}$$

$$+\mu_B(i,j)(1-\tau)c_t^{(B,M)}(i,j)p_t^B(i,j)\beta_{BM}\frac{S_t^B(i,j)I_t^M(i,j)}{N_t^B(i,j)} \tag{2}$$

$$I_{t+1}^B(i,j) = I_t^B(i,j) + \Lambda_t^I(i,j) - \left(d_t^B(i,j) + \alpha_B\right)I_t^B(i,j) - \Gamma_t^I(i,j) + \sigma_B E_t^B(i,j) - r_B I_t^B(i,j) \tag{3}$$

$$R_{t+1}^B(i,j) = R_t^B(i,j) + \Lambda_t^R(i,j) - \left(d_t^B(i,j) + l_B\right)R_t^B(i,j) - \Gamma_t^R(i,j) + r_B I_t^B(i,j) \tag{4}$$

$$D_{t+1}^B(i,j) = D_t^B(i,j) + \alpha_B I_t^B(i,j) \tag{5}$$

The total number of birds in cell (i,j) at time t is given by

$$N_t^B(i,j) = S_t^B(i,j) + E_t^B(i,j) + I_t^B(i,j) + R_t^B(i,j)$$

The total number of birds in the simulation area vary across the year following a seasonal trend represented in Fig. 4. The mean bird density during cold season is stable. During spring bird migratory and breeding season, the bird population increases to double the local cell density, it then stabilizes during the summer season. In fall migration season, the bird density decreases to reach the cold season density level. The birds leaving the simulation area during fall is a mix of susceptible and recovered bird, proportionally to the prevalence of each state in the population at the end of the summer season. The birds moving through the simulation area spend a part (τ) of the time step in each cell they move through.

The human epidemiological dynamic is given by equations (6) to (10)

$$S_{t+1}^H(i,j) = S_t^H(i,j) + b_t^H(i,j)S_t^H(i,j) - d_t^H(i,j)S_t^H(i,j) + l_H R_t^H(i,j) - c_t^{(H,M)}(i,j)p_t^H(i,j)\beta_{HM}\frac{S_t^H(i,j)I_t^M(i,j)}{N_t^H(i,j)} \tag{6}$$

$$E_{t+1}^H(i,j) = E_t^H(i,j) - d_t^H(i,j)E_t^H(i,j) + \sigma_H E_t^H(i,j) + c_t^{(H,M)}(i,j)p_t^H(i,j)\beta_{HM}\frac{S_t^H(i,j)I_t^M(i,j)}{N_t^H(i,j)} \tag{7}$$

$$I_{t+1}^H(i,j) = I_t^H(i,j) - \left(d_t^H(i,j) + \alpha_H\right)I_t^H(i,j) + \sigma_H E_t^H(i,j) - r_H I_t^H(i,j) \tag{8}$$

$$R_{t+1}^H(i,j) = R_t^H(i,j) - \left(d_t^H(i,j) + l_H\right)R_t^H(i,j) + r_H I_t^H(i,j) \tag{9}$$

$$D_{t+1}^H(i,j) = D_t^H(i,j) + \alpha_H I_t^H(i,j) \tag{10}$$

The total number of humans in cell (i,j) at time t

$$N_t^H(i,j) = S_t^H(i,j) + E_t^H(i,j) + I_t^H(i,j) + R_t^H(i,j)$$

And finally, the dynamics of the mosquitoes is governed by equations (11)–(13)

$$S_{t+1}^M(i,j) = S_t^M(i,j) + \Lambda_t^M(i,j) - d_t^M(i,j)S_t^M(i,j)$$

$$-(1 - \mu_B(i,j)) \; c_t^{(B,M)}(i,j)p_t^B(i,j)\beta_{BM}\frac{S_t^M(i,j)I_t^B(i,j)}{N_t^B(i,j)}$$

$$-\mu_B(i,j)\tau c_t^{(B,M)}(i,j)p_t^B(i,j)\beta_{BM}\sum_{(\alpha_k,\beta_k)\in N^*}d^{(\alpha_k,\beta_k)}(i,j)\frac{S_t^M(i,j)I_t^B(i+\alpha_k,j+\beta_k)}{N_t^B(i+\alpha_k,j+\beta_k)}$$

$$-\mu_B(i,j)(1 - \tau)c_t^{(B,M)}(i,j)p_t^B(i,j)\beta_{BM}\frac{S_t^M(i,j)I_t^B(i,j)}{N_t^B(i,j)} \tag{11}$$

$$E_{t+1}^M(i,j) = E_t^M(i,j) - d_t^M(i,j)E_t^M(i,j) - \sigma_M E_t^M(i,j)$$

$$+(1 - \mu_B(i,j))c_t^{(B,M)}(i,j)p_t^B(i,j)\beta_{BM}\frac{S_t^M(i,j)I_t^B(i,j)}{N_t^B(i,j)}$$

$$+\mu_B(i,j)\tau c_t^{(B,M)}(i,j)p_t^B(i,j)\beta_{BM}\sum_{(\alpha_k,\beta_k)\in N^*}d^{(\alpha_k,\beta_k)}(i,j)\frac{S_t^M(i,j)I_t^B(i+\alpha_k,j+\beta_k)}{N_t^B(i+\alpha_k,j+\beta_k)}$$

$$+\mu_B(i,j)(1 - \tau)c_t^{(B,M)}(i,j)p_t^B(i,j)\beta_{BM}\frac{S_t^M(i,j)I_t^B(i,j)}{N_t^B(i,j)} \tag{12}$$

$$I_{t+1}^M(i,j) = I_t^M(i,j) - d_t^M(i,j)I_t^H(i,j) + \sigma_M E_t^M(i,j) \tag{13}$$

The total number of mosquitoes in the simulation area vary across the year following a seasonal trend represented in Fig. 4. The mean mosquito density during cold season is zero. During the mosquito activity season, the mean mosquito density increases and then decreases to mimic observed mosquito seasonality under the latitude of the study region. Population increase is modeled by forcing inputs into compartment S of the mosquito population and population decrease occurs naturally due to the natural mortality of mosquitoes.

All the involved parameters in the model are detailed in Table 1.

2.5. Study area

Our study focused on a region in eastern Ontario, Canada and uses two study areas with the smallest being a subregion of the largest. The largest area is composed of five health units: the City of Ottawa ($\sim 2\,986\ Km^2$ with 1 017 449 inhabitants), Eastern Ontario ($\sim 5\,569\ Km^2$ with 210 276 inhabitants), Leeds, Grenville and Lanark district ($\sim 7\,052\ Km^2$ with 179 830 inhabitants), Renfrew county and district ($\sim 16\,945\ Km^2$ with 107 522 inhabitants) and Kingston, Frontenac and Lennox and Addington ($\sim 7\,480\ Km^2$ with 206 962 inhabitants) (StatCan, 2016, 2023). It covers about 40,032 Km^2 (Fig. 3). The smallest area is composed of a square lattice of 45x45 cells of 4 km^2 each (Fig. 3) and represents about 20.23% of our largest study area. It primarily covers the following urbanized centers: City of Ottawa (~1 million population), and a suite of villages and small towns such as North Grenville, North Dundas, Mississippi Mills, Rideau Lakes, and Carleton Place. The climate of the study region is humid continental (Euler et al., 2000), and land use is of mixed but primarily agricultural disposition with patches of forested land and a suite of urban centers (Butt et al., 2005; Rakotoarinia et al., 2022).

2.6. Model calibration

We used three databases to calibrate our model. The first one comes from the global bird monitoring project eBird (Sullivan et al., 2014) managed by the Cornell Lab of Ornithology. eBird is formed by a large network of birdwatchers around the world. Observers summarize their sighting data on a checklist that contains the name of the species observed, their number, date, location, method of observation and much more. The checklist is sent to eBird, which performs an initial set of checks. The checklist is accepted when the information is consistent with what is expected in the monitored area. However, when the information is unexpected for a particular location, eBird performs additional checks before accepting or rejecting it (Cornell Lab of Ornithology, Oct 2021; Sullivan et al., 2014).

One of our objectives was to identify cells with high bird abundance in our small study area which is our simulation area. Our approach was to collect all observation data (number of individuals, date, location, observation method, etc.) of American robin for our large study area from January 2010 to October 2021 (Cornell Lab of Ornithology, Oct 2021). Over the 12 years, the number of observations recorded is 168 278, which corresponds to 835 931 robins observed. We projected these observation locations onto our study areas in the Lambert Conformal Conic projection (North American Datum 1983 [NAD83]) using
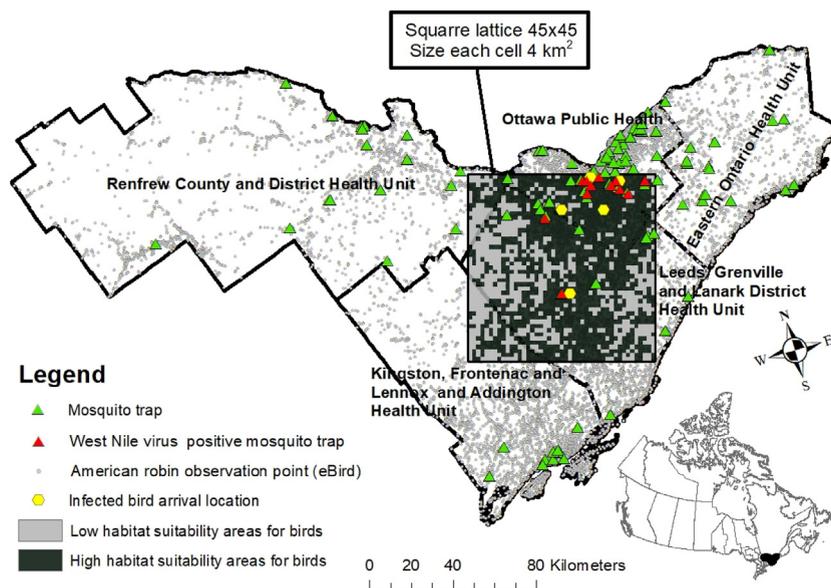
Fig. 3. Bird and mosquito observation area. This graphic was generated with a Lambert Conformal Conic projection (North American Datum 1983 [NAD83]) using observation data from June 2010 to October 2021.

ArcMap 10.8.2 software. Fig. 3 shows the spatial distribution of the observations. We then identified the locations of bird sightings in our simulation area.

This, first, allowed us to build a map that specifies the zones of high or low habitat suitability for birds. In 1330 cells (about 66%), robins were observed at least once during the period from June 2010 to October 2021. These are called the high habitat suitability areas for birds. No robins were observed in 695 cells (about 34%). These are referred to as low habitat suitability areas (see Fig. 3).

We then calculated the statistical parameters (the total number of observations and the average number of individuals observed per cell). We then selected the five cells with the highest number of bird observations and the highest average number of individuals observed. Limiting the number of cells to 5 was chosen for simplicity's sake, to enable us to better analyze each site where the epidemic starts. These cells designated A_i, $i \in \{1, ..., 5\}$ were our Exposed bird arrival locations (Fig. 3 (yellow hexagon) and Fig. 6). We also calculated the mean number of birds observed by week over the 12 years sequentially. The average trend of this time series as well as the boundaries of its variation during the season (min and max value (34 and 100)) allowed us to calibrate the bird density in our simulation (Fig. 4a).

The second source of data comes from the Breeding Bird Survey (BBS), a large-scale survey of North American birds whose main objective is to estimate the evolution of the populations of birds encountered along the roads. We calculated the average value of the annual abundance indices of the American robin estimated by the BBS for Ontario from 2010 to 2019 (Sauer et al., 2020) and used it to set the limit value of abundance over the breeding period (April 15 - July 31).

Using as a 'guide' the eBird and the BBS data, we calculated a curve of the seasonal variation of the expected densities of American robins within a cell. This variation considers in spring and early summer, an increase in density linked both to the arrival of migratory American robins and to births, then, in late summer and early autumn, a drop in population linked to the departure of migratory individuals. Natural mortality is also considered, but the overall trend is stable and around 50 individuals per 4 km^2 cell at the beginning of each year. Density variation is consistent with litter size and number as described in (Vanderhoff et al.).

The last source of data is from the WNV surveillance program of Public Health Ontario. This data allowed us to calibrate mosquito abundance variations in our simulation area as well as helped to identify zones of West Nile transmission for our model validation step (PHO, 2021).

The surveillance data used in our study was collected from 2010 to 2019 and corresponded to 4525 captures and 45 233 adult CPR mosquitoes (Fig. 3). We calculated the mean number of mosquitoes captured by week averaging the 10 years, for the simulation area. We then used this time series to calibrate the mosquito abundance in each of our cells. We then adjusted it to the observed abundance multiplied by 225 to account for the fact that trapped mosquitoes are only a sub-sample of the true mosquito population in an area. It is thus considered that each cell of 4 0000000 m^2 can contain 225 traps which will each cover approximately 17 778 m^2.

(a) Birds   (b) Mosquitoes
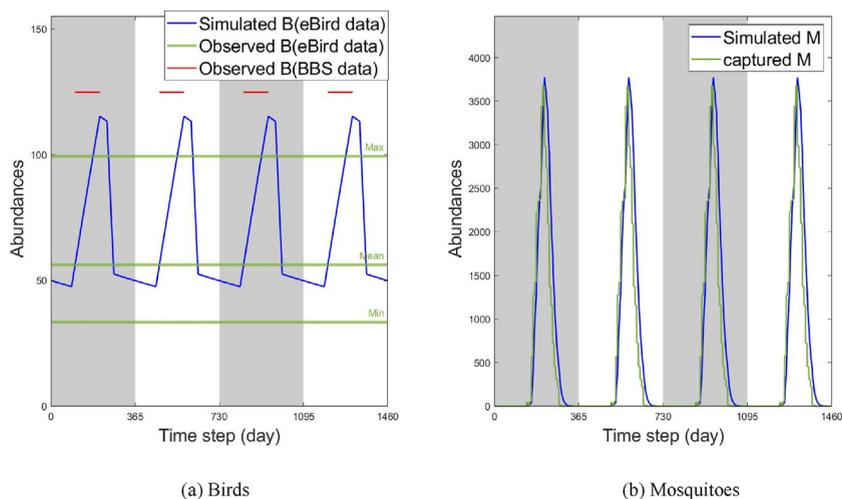
Fig. 4. (a) Simulated seasonal variation in abundance (blue line) and observed mean, minimum and maximum values of abundance, in our large study area for American robin based on eBird data (green line). Mean observed value in abundance in our large study area for American robin based on BBS data (red line). (b) Simulated (blue line) and observed (green line) seasonal variation in abundance in our large study area for *Culex pipiens-restuans* based on public health Ontario mosquito surveillance data.

2.7. Model validation

We simulated the spatial spread of WNV for birds, mosquitoes, and humans in our simulation zone. We represented the spatial and temporal evolution of the number of infected individuals in birds. We than compared visually the areal coherence of WNV transmission in bird populations obtained in our simulation with the location of the WNV positive CPR mosquito traps obtained between 2010 and 2019 from the Ontario mosquito-borne disease surveillance program.

2.8. Sensitivity analysis

We performed sensitivity analyses of our model for birds, mosquitoes, and humans. The outputs considered in the simulation area were the total number of newly infected individuals, maximum number of infectious individuals and the time of this maximum. We evaluated for each category of agents, the sensitivity of the outputs to a 5% increase and decrease of all parameters of our model. Separately for each parameter, we calculated the outputs values for a simulation using its mean value, the mean value + 5% increase and the mean - 5% decrease. It made 17 parameters * 3 sensitivity scenarios (mean, +5%, −5%) * 3 outputs simulations to run. We than represented the results in histogram to detect global and specific effect of the parameters values variation visually.

3. Result

3.1. Model validation

In this section, we simulate WNV transmission and compare it visually with the observed locations of the WNV mosquito positive traps.

3.1.1. WNV transmission due to arrival of infected birds from spring migration

We simulated a WNV epidemic over 10 years in our simulation area. Fig. 5 shows the global dynamics of the evolution of the epidemic in bird, mosquito, and human populations.

Each year, about 107 531 birds arrive in all our cells in spring, for each cell of our simulation area for 10 years (see Fig. 1). Among them, 97 365 of which arrive in the high suitability areas and the rest in the low suitability areas. During the first year only, about 92 WNV infected birds arrive in the 5 predefined cells (see Fig. 3), distributed evenly between day 121 (May 1) and day 181 (June 30).

Bird populations fluctuate seasonally. The population of the susceptible increases from day 91 (April 1), reaches its maximum in late spring (day 212 (July 31)) and then decreases. The same pattern is observed over the 10 years of simulation (Fig. 5). Following the arrival of infected birds, the first year of simulation, local transmission of WNV starts to spread across the simulation area. The total number of newly infected for the first year after introduction of the virus is 810. Among them

(a) Birds

(b) Humans
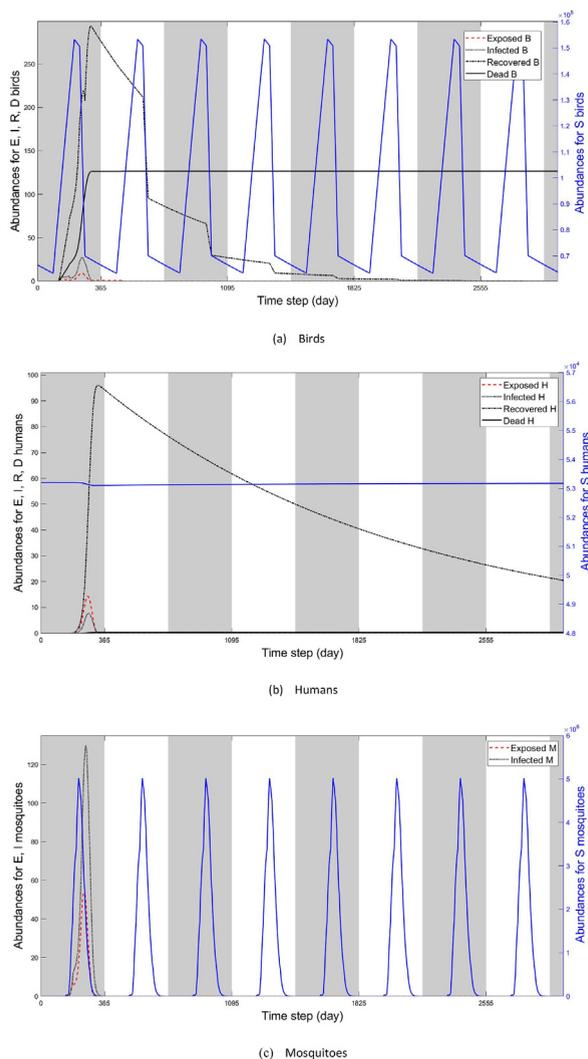
(c) Mosquitoes

Fig. 5. Global dynamics of (a) birds, (b) humans, and (c) mosquitoes in the simulation area. Abundances are the total number of exposed (E), infected (I), recovered (R) or dead (D) individuals for birds and humans. For mosquitoes, abundances are the total number of exposed (E) or infected (I) individuals.

624 are in high habitat suitability areas for birds. The maximum number of infected birds is 38 and is reached on day 258 (September 15).

Mosquito populations evolve following regular seasonal waves, much as do the birds. The maximum abundance is during summer (day 217 – August 5). No active mosquitoes are observed between day 304 (October 31) and day 137 (May 17). The same pattern was observed over the 10 years of simulation (Fig. 5). During the first year after virus introduction, there was a total number of 1179 infected mosquitos. The maximum number of infected individuals is 247 on day 258 (September 15), paralleled with the bird population (Fig. 5).

The human population remains globally stable in the study region, with a slight decrease in the first year due to the epidemic. The total number of newly infected humans is 178 for the first year after the introduction of the virus, with a maximum of 14 on day 275 (October 2), 2 weeks after the maximum in bird and mosquito (Fig. 5). The total number of recovered individuals increases and reaches its maximum on day 306 (November 2) (Fig. 5).

3.1.2. Comparison between areas of WNV transmission in bird populations and mosquito positives pools

We visually compared the transmission area of our previous simulations with the location of the WNV-positive mosquito traps (see Fig. 6).

There is a good overlap between transmission areas in birds and mosquito traps in areas A_1, A_2, and A_5. The correspondence is less clear for areas A_3 and A_4 (see Fig. 6 and Table 2). According to our analysis, there are two possible explanations for

Table 2
Comparison between areas of WNV transmission in bird populations and WNV mosquito positive traps.

Simulated areas of WNV transmission in bird populations	Observed locations of the WNV mosquito positive traps	Overlap between WNV mosquito positive traps and simulated areas of WNV transmission in bird populations
A1	Within a radius of $\sim$ 12 km around A1, we have around 5 WNV mosquito positive traps. The nearest positive trap is $\sim$ 3 km away. We have 2 others at $\sim$ 4 km, 1 at $\sim$ 5 km and the last one at $\sim$ 9 km.	Strong
A2	Within a radius of $\sim$ 12 km around A2, we have around 5 WNV mosquito positive traps. The nearest positive trap is $\sim$ 2 km away. We have 2 others at $\sim$ 5 km, 1 at $\sim$ 8 km and the last one at $\sim$ 10 km.	Strong
A3	Within a radius of $\sim$ 12 km around A3, we have only 1 WNV mosquito positive trap at $\sim$ 10 km	weak
A4	Within a radius of $\sim$ 12 km around A4, we have only 1 WNV mosquito positive trap at $\sim$ 11 km	weak
A5	Within a radius of $\sim$ 12 km around A5, we have 1 WNV mosquito positive trap but at $\sim$ 4 km	Strong
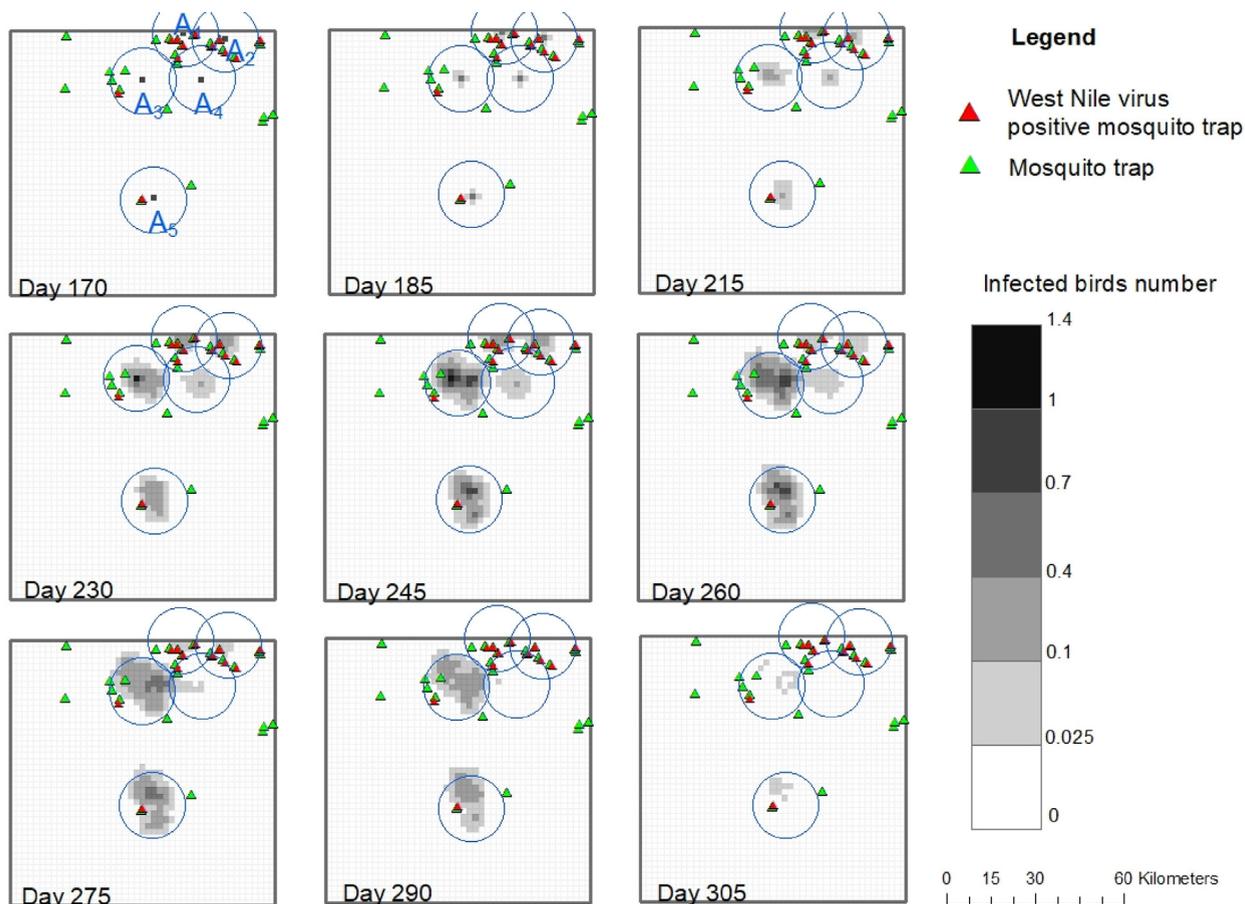
Fig. 6. Comparison of WNV spread and WNV positive mosquito traps for bird species in the simulation area. $A_1, A_2,...$ and A_5 represent the 5 predefined cells in with infected birds arrive.

this mismatch. The first could be linked to the spatial distribution of the mosquito traps. They are not covering our simulation area homogeneously. The trap closest to the center of area A_3 is at least 6 km away and the trap at point A_4 is at least 9 km away. Thus, there are no traps to confirm if there is actually transmission or not in region A3 and A4. We hypothesized it could be the case as eBird data show high American robin density at these locations.

The second explanation could be linked to the assumptions that led to the selection of the 5 arrival cells for infected birds. Indeed, our 5 cells represent those with the highest number of sightings and individuals observed according to the eBird data.

But infected birds might actually arrive somewhere else too. Other locations where infected birds arrive could easily be tested in the future.

3.2. Sensitivity analysis

Sensitivity analysis in the low and high bird suitability areas and across the simulation area for all categories of agents showed the same trend after a 5% increase or decrease in each parameter (see the 27 graphs in the supplementary material) for the total number of newly infected individuals, the maximum of infectious individuals and the time of this maximum.

The sensitivity analysis also showed that a small variation (-5% or $+5\%$) in the parameters rate of biting of bird by mosquito ($c^{(B,M)}$), end time of arrival of the birds, mosquito natural mortality rate (d^M), per contact probability of transmission from mosquito to bird and form bird to mosquito (β_{BM} and β_{MB}) and recovery rate for bird (r_B), in our simulation area, has some impact on the total number of newly infected birds, humans or mosquitoes. The variation of the other parameters has almost no effect on this number (see Fig. 7 graphs (a)-(b)-(c)). The sensitivity analysis then showed that a 5% increase or decrease in the parameters $c^{(B,M)}$ and d^M, in our simulation area has a more important impact on the maximum of infectious birds, humans and mosquitoes than the other parameters. In contrast, varying the parameters end time of arrival of the birds, β_{MB}, β_{BM} r_B, and incubation period for mosquitoes ($1/\sigma_M$) has the least impact on it (See Fig. 7 graphs (d)-(e)–(f)). Variation in end time of arrival of the birds, d^M, r_B, recovery rate for human (r_H), $c^{(B,M)}$, incubation period for human ($1/\sigma_H$) et $1/\sigma_M$ increases and decreases the time of the maximum infectious individuals by 1 or 2 days in all agents in the simulation area. No change was observed in the time of the maximum infectious individuals when we varied the other parameters of our model (see Fig. 7 graphs (g)-(h)–(i)).

In summary, the sensitivity analysis showed that a 5% increase or decrease in each parameter of our model, except for $c^{(B,M)}$ and d^M, had a very limited effect on the total number of newly infected individuals (birds, humans, and mosquitoes) or on the maximum number of infectious individuals or onset date. Variations in $c^{(B,M)}$ and d^M had a greater impact on the maximum number of infectious individuals. Therefore, values for these parameters should be chosen with caution.

4. Conclusion

Modeling is an essential tool for understanding the dynamics of the spread of infectious diseases and assessing the risk they pose to human and animal health. In this work, we built a spatial modeling tool for West Nile Virus transmission in eastern Ontario using the cellular automaton approach. This tool was designed to explore various factors suspected to be responsible for the periodic re-emergence of WNV in our study area. These factors included periodic introduction of infected reservoir hosts [especially during spring bird migration season], population movements of hosts and vectors during the transmission season, changes in vector feeding preferences during the transmission season, and persistence of infected vectors on the territory during the winter. In the present work, only the spatial heterogeneity of the reservoir hosts (birds) and the hypothesis of the arrival of infected birds in spring in the simulation area were explored. The transmission maps generated corresponded reasonably well with existing transmission areas that were observed between 2010 and 2019 via entomological surveillance. This historical validation element demonstrates utility of the developed model to successfully describe the spread of WNV in Ontario. The comparison of simulated results and observations, suggests that other factors explain the periodic re-emergence of the virus in our study area; hence our model is heuristic regarding its capacity to identify the most important predictor criteria.

The sensitivity analysis of the 17 parameters of our model showed its robustness, even if some parameters (rate of biting of bird by mosquito ($c^{(B,M)}$) and mosquito natural mortality rate (d^M) need to be chosen with caution.

Finally, the tool developed here is a deterministic model. It simulates epidemics according to a central tendency given to the different parameters of the model. Given the limited number of individuals (especially birds) in each cell, it will therefore tend to overestimate the risk of an epidemic since it considers that even a fraction of infected birds is viable, which is not the case in a stochastic model. Other limitations of our model include the assumption that humans (accidental hosts) do not move between cells, that their density is homogeneous across the study region, and that our choice of limiting the arrival of infected birds to 5 cells is arbitrary. These limitations were founded in attempts to reduce model complexity, and for allowing a clearer analysis of the model. Indeed, modeling the mobility of human beings is not an essential element to add to our model, since most of the bites made by the virus vector in our study region are usually conducted in the evening, when individuals are usually back home. However, the addition of a heterogeneous distribution of human population densities would be very interesting in future studies, as it would allow us to better assess the impact of epidemics on human populations and carry out 'burden of diseases studies' under different scenarios. Additionally, the arrival of infected birds in a cell chosen at random, and the repetition of the experiment a significant number of times, provides an avenue for studying the epidemics possibly initiated by the arrival of infected birds in the region of study.

This tool will also allow us to study the impact of climate change/land use change on West Nile Virus transmission using direct and indirect variables climate driving variables. Indeed, the model could be used to explore scenarios of changes in
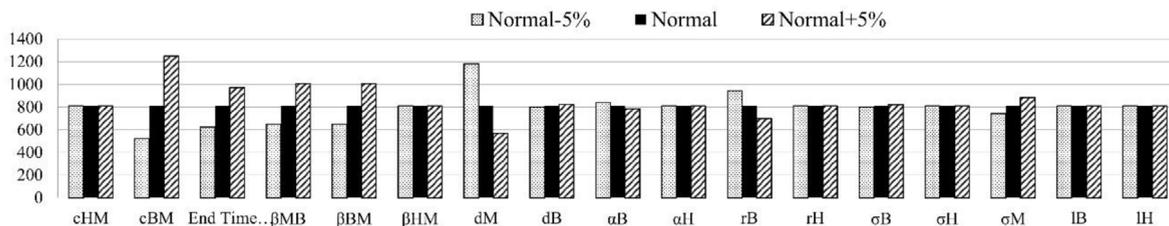
(a) Total number of newly infected birds in the simulation area.
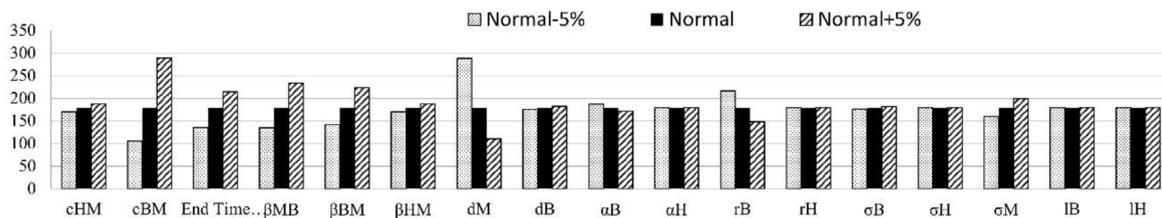
(b) Total number of newly infected humans in the simulation area
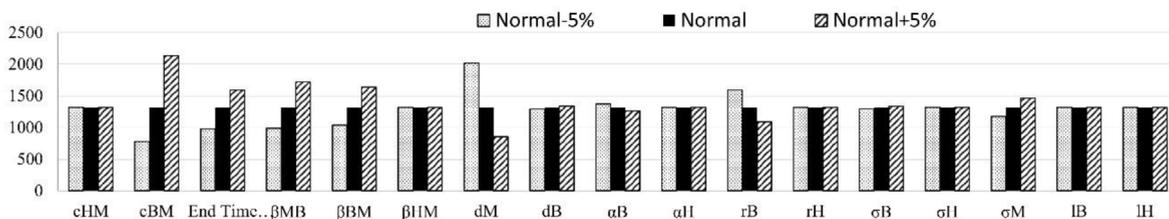
(c) Total number of newly infected mosquitoes in the simulation area
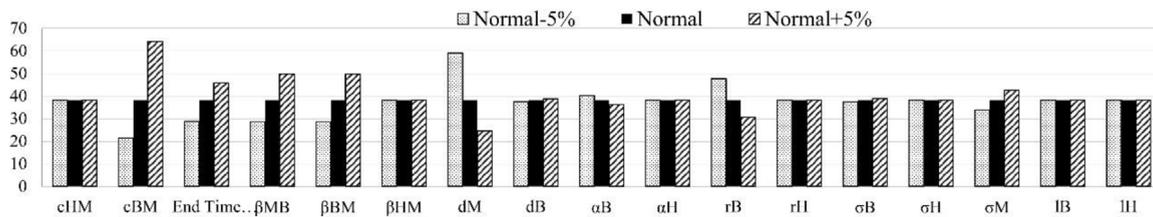
(d) Maximum number of infectious birds in the simulation area

Fig. 7. Graphs (a), (b), and (c) represent the change in the total number of newly infected birds, humans, and mosquitoes, respectively, in the simulation area following a 5% increase or decrease in each parameter of our model. Graphs (d), (e), and (f) represent the change in the maximum number of infectious birds, humans, and mosquitoes, respectively, in the simulation area after a 5% increase or decrease in each parameter of our model. Graphs (g), (h) and (i) represent the change in the time of onset of these maxima in birds, humans and mosquitoes respectively, in the simulation area following a 5% increase or decrease in each parameter of our model. The term "normal" is used to designate the estimated value in Table 1.

vector and host abundance, decreases in the extrinsic incubation period of vectors, and changes in the behavior and mobility of human populations in the context of environmental and anthropogenic changes. The specific simulations produced in this study also allow us to provide public health decision makers with information to better understand and prevent the risk of WNV transmission in eastern Canada; a region experiencing rapid changes in conditions suitable for WNV proliferation.
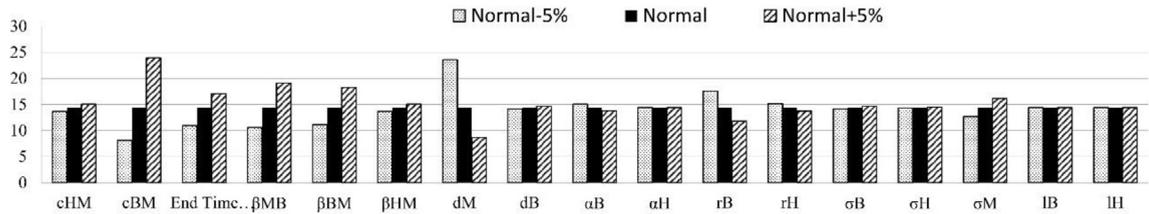
(e) Maximum number of infectious humans in the simulation area
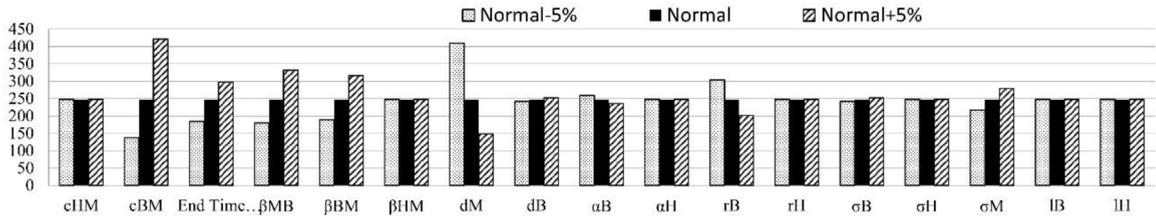
(f) Maximum number of infectious mosquitoes in the simulation area
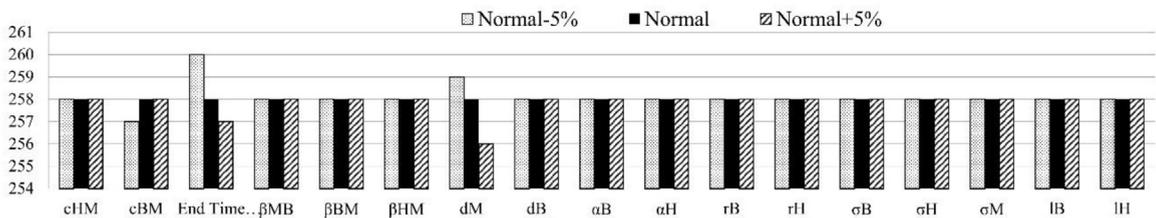
(g) Time of maximum number of infectious birds in the simulation area
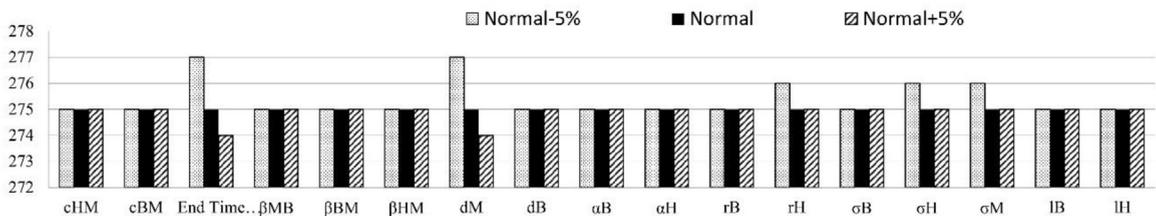
(h) Time of maximum number of infectious humans in the simulation area
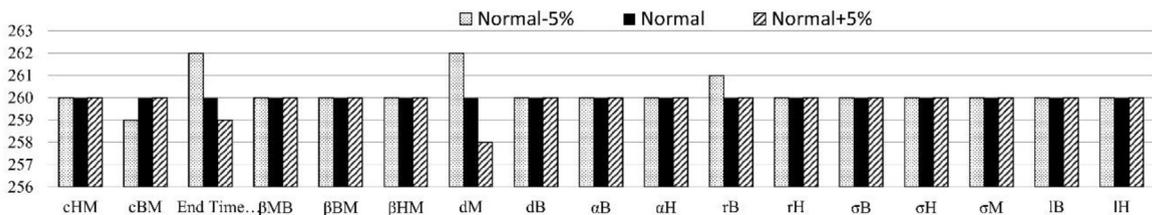
(i) Time of maximum number of infectious birds in the simulation area

Fig. 7. (*continued*).

Authors' contributions

Baki Cissé: Conceptualization, Methodology, Software, Formal analysis, Data curation, Writing - Original Draft; David R Lapen: Conceptualization, Writing - Review & Editing; Funding acquisition; Nick H. Ogden: Conceptualization, Methodology, Writing - Review & Editing; Funding acquisition; K. Chalvet-Monfray: Conceptualization, Methodology, Writing - Review & Editing; Antoinette Ludwig: Conceptualization, Methodology, Software, Formal analysis, Writing - Original Draft, Supervision, Funding acquisition;

CRediT authorship contribution statement

Baki Cissé: Conceptualization, Data curation, Formal analysis, Methodology, Software, Writing — original draft. **David R. Lapen:** Conceptualization, Funding acquisition, Writing — review & editing. **K. Chalvet-Monfray:** Conceptualization, Methodology, Writing — review & editing. **Nicholas H. Ogden:** Conceptualization, Funding acquisition, Methodology, Writing — review & editing. **Antoinette Ludwig:** Conceptualization, Formal analysis, Funding acquisition, Methodology, Software, Supervision, Writing — original draft.

Declaration of competing interest

The authors declare that they have no known competing financial interests or personal relationships that could have appeared to influence the work reported in this paper.

Appendix A. Parameter estimation

A.1. Estimation of $c^{(B,M)}$ and $c^{(M,B)}$

We assume that:

$c^{(B,M)} = c^{(M,B)}$ (Wonham et al., 2004)

In an experimental study [80] (Table 2), birds (jackdaws and house sparrows) were placed in cages in the presence of *Culex. Pipiens*. Some of the results are summarized in the table below.

Table A.2

Bird species	No. of mosquitoes in each assay per box (mean ± SE)	No. of engorged mosquitoes per box (mean ± SE)
Jackdaws	49.7 ± 6.2	3.6 ± 1.0
House sparrow	53.0 ± 7.7	6.9 ± 1.3

The effective biting rate of CPR on a bird (jackdaws and house sparrows) is.
$c^{(M,B)} = ((3.6 / 49.7) + (6.9 / 53)) / 2 = 0.10$ for 30 *minutes* (Gutiérrez-López et al., 2019).
Yet the CPR is an active mosquito at the end of the day for approximately 1 h (Ryan et al., 2017). Therefore, the daily biting rate

$$t_{day} = 2 \times t_{30 \ min} = 0.2 \tag{A.4}$$

As 55.3% of blood meals collected from birds are from American robin (Khalil et al., 2021), therefore $c^{(B,M)} = c^{(M,B)} = 0.2 \times 0.553 \approx 0.11/day$. (A.1)

A.2. Estimation of $c^{(H,M)}$ and $c^{(M,H)}$

We assume that:

$c^{(H,M)} = c^{(M,H)}$

The rate of biting of human by mosquito (CPR) is approximately 0.08 per 25 min of a night of capture [70]. As the CPR is an active mosquito at the end of the day for approximately 1 h (Ryan et al., 2017). Therefore, the daily biting rate

$$c^{(H,M)} = 2.4 \times 0.08 = 0.192 \tag{A.2}$$

A.3. Mosquito feeding rate

The mosquitoes feeding preferences to the two types of hosts (humans and birds) is less than 1, i.e. $p^B + p^H < 1$. This is because mosquitoes can feed on other mammals (Abdelrazec et al., 2014). (A.3)

A.4. Human birth rate b^H

The crude birth rate, or the number of live births per 1000 population, was 9.3 for Ontario in 2020 (StatCan, 2022a).

$$\text{Therefore}, b^H = \frac{9.5}{1000 \times 365} \approx 0.00003 \tag{A.4}$$

A.5. Human natural death rate d^H

Human death rate per 1000 population, was 7.8 for Ontario in 2020 (StatCan, 2022b).

$$\text{Therefore}, d^H = \frac{7.8}{1000 \times 365} \approx 0.0000214 \tag{A.5}$$

A.6. Pathogen virulence to infectious human α_H

The overall case fatality rate ranges from 4% to 14% in individuals exhibiting neuroinvasive disease (PHAC, 2010).
Very few people (less than 1% of those infected with the virus) will develop severe symptoms and health effects. Some severe cases of the disease can be fatal (PHAC, 2015).
Therefore, Pathogen virulence to infectious human is estimated to be

$$9\% \text{ (mean value)} \times 1\% = 0.0009 \tag{A.6}$$

A.7. Recovery rate for human r_H

West Nile fever is typically a mild illness lasting 3—6 days (PHAC, 2010). Therefore, recovery rate for human is estimated to be $1/4.5 = 0.22$ (mean value). (A.7)

A.8. Incubation period for human $1/\sigma_H$

First symptoms usually appear within 2—15 days after infection (PHAC, 2015). Therefore, recovery rate for human is estimated to be 8.5 (mean value). (A.8)

Appendix B

Abbreviation/word	Description
WNV	West Nile Virus
CA	Cellular Automata
CPR	*Culex pipiens-restuans*
SEIRDS - SEI	Susceptible, Exposed, Infectious, Recovered, Dead - Susceptible, Exposed, Infectious
VBDs	Vector-Borne Diseases
CFIA	Canadian Food Inspection Agency
PHAC	Public Health Agency of Canada
eBird	Global bird monitoring project
BBS	Breeding Bird Survey
NAD83	North American Datum 1983

Appendix C. Supplementary data

Supplementary data to this article can be found online at https://doi.org/10.1016/j.idm.2024.01.002.

References

Abdelrazec, A., Lenhart, S., & Zhu, H. (2014). Transmission dynamics of West Nile virus in mosquitoes and corvids and non-corvids. *Journal of Mathematical Biology, 68*(6), 1553–1582. https://doi.org/10.1007/s00285-013-0677-3

Andreadis, T. G. (2012). The contribution of Culex pipiens complex mosquitoes to transmission and persistence of West Nile virus in North America. *Journal of the American Mosquito Control Association, 28*(4s), 137–151.

Badawi, A., Velummailum, R., Ryoo, S. G., Senthinathan, A., Yaghoubi, S., Vasileva, D., Ostermeier, E., Plishka, M., Soosaipillai, M., & Arora, P. (2018). Prevalence of chronic comorbidities in dengue fever and West Nile virus: A systematic review and meta-analysis. *PLoS One, 13*(7), Article e0200200. https://doi.org/10.1371/journal.pone.0200200 [Review].

Belkhiria, J., Alkhamis, M. A., & Martínez-López, B. (2016). Application of species distribution modeling for avian influenza surveillance in the United States considering the North America migratory flyways. *Scientific Reports, 6*(1), Article 33161.

Bowman, C., Gumel, A., Van den Driessche, P., Wu, J., & Zhu, H. (2005). A mathematical model for assessing control strategies against West Nile virus. *Bulletin of Mathematical Biology, 67*(5), 1107–1133.

Brugman, V. A., England, M. E., Stoner, J., Tugwell, L., Harrup, L. E., Wilson, A. J., Medlock, J. M., Logan, J. G., Fooks, A. R., & Mertens, P. P. (2017). How often do mosquitoes bite humans in southern england? A standardised summer trial at four sites reveals spatial, temporal and site-related variation in biting rates. *Parasites & Vectors, 10*, 1–11.

Buonomo, B., Chitnis, N., & d'Onofrio, A. (2018). Seasonality in epidemic models: A literature review. *Ricerche di Matematica, 67*, 7–25.

Butt, S., Ramprasad, P., & Fenech, A. (2005). Changes in the landscape of southern Ontario Canada since 1750: Impacts of European colonization. *Integrated mapping assessment*, 83–92.

Canada, G. o. Mosquito-borne diseases national surveillance report. https://www.canada.ca/en/public-health/services/diseases/west-nile-virus/west-nile-virus-other-mosquito-borne-disease.html#y2018. (Accessed 28 April 2023).

CDC. (2021). Centers for Disease Control and Prevention)West Nile virus transmission. https://www.cdc.gov/westnile/transmission/index.html. (Accessed 12 May 2023).

Ciota, A. T., Drummond, C. L., Ruby, M. A., Drobnack, J., Ebel, G. D., & Kramer, L. D. (2012). Dispersal of Culex mosquitoes (Diptera: Culicidae) from a wastewater treatment facility. *Journal of Medical Entomology, 49*(1), 35–42.

Cissé, B., El Yacoubi, S., & Gourbière, S. (2016a). A cellular automaton model for the transmission of Chagas disease in heterogeneous landscape and host community [Article]. *Applied Mathematical Modelling, 40*(2), 782–794. https://doi.org/10.1016/j.apm.2015.10.030

Cissé, B., El Yacoubi, S., & Gourbière, S. (2016b). The spatial reproduction number in a cellular automaton model for vector-borne diseases applied to the transmission of Chagas disease. *Simulation, 92*(2), 141–152. https://doi.org/10.1177/0037549715626520

Cissé, B., El Yacoubi, S., & Tridane, A. (2013). Impact of neighborhood structure on epidemic spreading by means of cellular automata approach. *Procedia Computer Science, 18*, 2603–2606.

Cissé, B., Yacoubi, S. E., & Gourbière, S. (2014). The basic reproduction number for chagas disease transmission using cellular automata. In *Lecture notes in computer science (including subseries lecture notes in artificial intelligence and lecture notes in bioinformatics)* (Vol. 8751, pp. 278–287).

Cornell Lab of Ornithology, I. (2021). *eBird basic dataset*. New York. *Version: EBD_relOct-2021* https://ebird.org/home. (Accessed 2 December 2022).

Cruz-Pacheco, G., Esteva, L., Montano-Hirose, J. A., & Vargas, C. (2005). Modelling the dynamics of West Nile Virus. *Bulletin of Mathematical Biology, 67*(6), 1157–1172. https://doi.org/10.1016/j.bulm.2004.11.008

Dohm, D. J., O'Guinn, M. L., & Turell, M. J. (2002). Effect of environmental temperature on the ability of Culex pipiens (Diptera: Culicidae) to transmit West Nile virus. *Journal of Medical Entomology, 39*(1), 221–225. https://doi.org/10.1603/0022-2585-39.1.221

Doran, R. J., & Laffan, S. W. (2005). Simulating the spatial dynamics of foot and mouth disease outbreaks in feral pigs and livestock in Queensland, Australia, using a susceptible-infected-recovered cellular automata model. *Preventive Veterinary Medicine, 70*(1–2), 133–152. https://doi.org/10.1016/j.prevetmed.2005.03.002

Durand, B., Balança, G., Baldet, T., & Chevalier, V. (2010). A metapopulation model to simulate West Nile virus circulation in Western Africa, Southern Europe and the Mediterranean basin. *Veterinary Research, 41*(3), 32.

Euler, D., Perera, A. H., & Thompson, I. D. (2000). *Ecology of a managed terrestrial landscape: Patterns and processes of forest landscapes in Ontario*. UBC Press.

Ewing, D. A., Purse, B. V., Cobbold, C. A., & White, S. M. (2021). A novel approach for predicting risk of vector-borne disease establishment in marginal temperate environments under climate change: West Nile virus in the UK. *Journal of The Royal Society Interface, 18*(178), Article 20210049. https://doi.org/10.1098/rsif.2021.0049

Farner, D. S. (1949). Age groups and longevity in the American Robin: comments, further discussion, and certain revisions. *The Wilson Bulletin*, 68–81.

Fasano, A., Riccetti, N., Angelou, A., Gomez-Ramirez, J., Ferraccioli, F., Kioutsioukis, I., & Stilianakis, N. I. (2022). An epidemiological model for mosquito host selection and temperature-dependent transmission of West Nile virus. *Scientific Reports, 12*(1), Article 19946. https://doi.org/10.1038/s41598-022-24527-5

Gutiérrez-López, R., Martínez-de la Puente, J., Gangoso, L., Soriguer, R., & Figuerola, J. (2019). Effects of host sex, body mass and infection by avian Plasmodium on the biting rate of two mosquito species with different feeding preferences. *Parasites & Vectors, 12*, 1–10.

Hirth, D. H., Albert, E. H., & Greeley, F. (1969). Dispersal and Flocking of Marked Young Robins (Turdus M. Migratorius) after Fledging. *Bird-Banding, 40*(3), 208–215. https://doi.org/10.2307/4511580

Jones, C. E., Lounibos, L. P., Marra, P. P., & Kilpatrick, A. M. (2012). Rainfall influences survival of Culex pipiens (Diptera: Culicidae) in a residential neighborhood in the mid-Atlantic United States. *Journal of Medical Entomology, 49*(3), 467–473.

Kari, J. (2005). Theory of cellular automata: A survey. *Theoretical Computer Science, 334*(1), 3–33. https://doi.org/10.1016/j.tcs.2004.11.021

Khalil, N., Little, E. A., Akaratovic, K. I., Kiser, J. P., Abadam, C. F., Yuan, K. J., Misencik, M. J., Armstrong, P. M., & Molaei, G. (2021). Host Associations of Culex pipiens: A Two-Year Analysis of Bloodmeal Sources and Implications for Arboviral Transmission in Southeastern Virginia. *Vector Borne and Zoonotic Diseases, 21*(12), 961–972.

Kilpatrick, A. M., Daszak, P., Jones, M. J., Marra, P. P., & Kramer, L. D. (2006). Host heterogeneity dominates West Nile virus transmission [Article]. *Proceedings of the Royal Society B: Biological Sciences, 273*(1599), 2327–2333. https://doi.org/10.1098/rspb.2006.3575

Komar, N., Langevin, S., Hinten, S., Nemeth, N., Edwards, E., Hettler, D., Davis, B., Bowen, R., & Bunning, M. (2003). Experimental infection of North American birds with the New York 1999 strain of West Nile virus. *Emerging Infectious Diseases, 9*(3), 311.

Kulkarni, M. A., Lecocq, A. C., Artsob, H., Drebot, M. A., & Ogden, N. H. (2013). Epidemiology and aetiology of encephalitis in Canada, 1994–2008: a case for undiagnosed arboviral agents? *Epidemiology and Infection, 141*(11), 2243–2255. https://doi.org/10.1017/S095026881200252X

Lin, Z., & Zhu, H. (2017). Spatial spreading model and dynamics of West Nile virus in birds and mosquitoes with free boundary. *Journal of Mathematical Biology, 75*(6–7), 1381–1409. https://doi.org/10.1007/s00285-017-1124-7

Ludwig, A., Bigras-Poulin, M., Michel, P., & Bélanger, D. (2010). Risk factors associated with west nile virus mortality in american crow populations in southern quebec [Article]. *Journal of Wildlife Diseases, 46*(1), 195–208. https://doi.org/10.7589/0090-3558-46.1.195

Ludwig, A., Zheng, H., Vrbova, L., Drebot, M. A., Iranpour, M., & Lindsay, L. R. (2019). Increased risk of endemic mosquito-borne diseases in Canada due to climate change. *Canada Communicable Disease Report, 45*(4), 91–97. https://doi.org/10.14745/ccdr.v45i04a03

Mallya, S., Sander, B., Roy-Gagnon, M. H., Taljaard, M., Jolly, A., & Kulkarni, M. A. (2018). Factors associated with human West Nile virus infection in Ontario: a generalized linear mixed modelling approach. *BMC Infectious Diseases, 18*(1), 141. https://doi.org/10.1186/s12879-018-3052-6

Mange, D., & Tomassini, M. (1998). *Bio-inspired computing machines: Towards novel computational architectures*. PPUR presses polytechniques.

Margolus, N. (1984). Physics-like models of computation. *Physica D: Nonlinear Phenomena, 10*(1), 81–95. https://doi.org/10.1016/0167-2789(84)90252-5

Mathieu, K., & Karmali, M. (2016). Vector-borne diseases, climate change and healthy urban living: Next steps. *Canada Communicable Disease Report, 42*(10), 219–221. https://doi.org/10.14745/ccdr.v42i10a13

Mikler, A. R., Venkatachalam, S., & Abbas, K. (2005). Modeling infectious diseases using global stochastic cellular automata. *Journal of Biological Systems, 13*(4), 421–439.

Moua, Y., Kotchi, S. O., Ludwig, A., & Brazeau, S. (2021). Mapping the habitat suitability of west nile virus vectors in southern Quebec and eastern Ontario, Canada, with species distribution modeling and satellite earth observation data [Article]. *Remote Sensing, 13*(9). https://doi.org/10.3390/rs13091637. Article 1637.

Nemeth, N. M., Oesterle, P. T., & Bowen, R. A. (2009). Humoral immunity to West Nile virus is long-lasting and protective in the house sparrow (Passer domesticus). *The American Journal of Tropical Medicine and Hygiene, 80*(5), 864. https://www.ncbi.nlm.nih.gov/pmc/articles/PMC2693945/pdf/nihms-119015.pdf.

Neumann, J.v. (1966). *Theory of self-reproducing automata*. Burks: Arthur W.

Oliver, R. Y., Mahoney, P. J., Gurarie, E., Krikun, N., Weeks, B. C., Hebblewhite, M., Liston, G., & Boelman, N. (2020). Behavioral responses to spring snow conditions contribute to long-term shift in migration phenology in American robins. *Environmental Research Letters, 15*(4), Article 045003. https://doi.org/10.1088/1748-9326/ab71a0

Ouhoumanne, N., Lowe, A. M., Fortin, A., Kairy, D., Vibien, A., K-Lensch, J., Tannenbaum, T. N., & Milord, F. (2018). Morbidity, mortality and long-term sequelae of West Nile virus disease in Québec [Article]. *Epidemiology and Infection, 146*(7), 867–874. https://doi.org/10.1017/S0950268818000687

PHAC. (2010). Pathogen Safety Data Sheets: Infectious Substances — West Nile virus (WNV). https://www.canada.ca/en/public-health/services/laboratory-biosafety-biosecurity/pathogen-safety-data-sheets-risk-assessment/west-nile-virus.html. (Accessed 16 February 2023).

PHAC. (2015). *Symptoms of West Nile virus*. https://www.canada.ca/en/public-health/services/diseases/west-nile-virus/symptoms-west-nile-virus.html. (Accessed 16 February 2023).

PHAC. (2021). *Mosquito-borne disease surveillance report: Biweekly edition (Week 39 to 42), Ottawa, Canada* https://www.canada.ca/en/public-health/services/publications/diseases-conditions/west-nile-virus-surveillance/2021/week-39-42-september-27-october-24.html.

PHO. (2021). *Ontario agency for health protection and promotion (public health Ontario). PHO mosquito database. Mosquito surveillance 2010 to 2019: (City of Ottawa (3551), eastern Ontario (3558), Leeds, Grenville and Lanark district (3543), Renfrew county and district (3557) and Kingston, frontenac and Lennox and Addington (3541).* https://www.publichealthontario.ca/fr/data-and-analysis/using-data/data-requests.

Rakotoarinia, M. R., Guillaume Blanchet, F., Gravel, D., Lapen, D. R., Leighton, P. A., Ogden, N. H., & Ludwig, A. (2022). Effects of land use and weather on the presence and abundance of mosquito-borne disease vectors in a urban and agricultural landscape in Eastern Ontario, Canada [Article]. *PLoS One, 17*(3 March), Article e0262376. https://doi.org/10.1371/journal.pone.0262376

Rappole, J. H., Derrickson, S. R., & Hubalek, Z. (2000). Migratory birds and spread of West Nile virus in the Western Hemisphere. *Emerging Infectious Diseases, 6*(4), 319.

Reisen, W. K., & Wheeler, S. S. (2019). Overwintering of West Nile Virus in the United States. *Journal of Medical Entomology, 56*(6), 1498–1507. https://academic.oup.com/jme/article-abstract/56/6/1498/5572361?redirectedFrom=fulltext.

Ripoche, M., Campagna, C., Ludwig, A., Ogden, N. H., & Leighton, P. A. (2019). Short-term Forecasting of Daily Abundance of West Nile Virus Vectors Culex pipiens-restuans (Diptera: Culicidae) and Aedes vexans Based on Weather Conditions in Southern Québec (Canada) [Article]. *Journal of Medical Entomology, 56*(3), 859–872. https://doi.org/10.1093/jme/tjz002

Robert, M., Hachey, M., Lepage, D., & Couturier, A. (2019). *Second atlas of the breeding birds of southern Quebec. Montreal, QC: Regroupement québec oiseaux. Canadian wildlife service (environment and climate change Canada), and bird studies Canada.*

Ruhomally, Y. B., Mungur, M., Khoodaruth, A. A. H., Oree, V., & Dauhoo, M. Z. (2022). Assessing the Impact of Contact Tracing, Quarantine and Red Zone on the Dynamical Evolution of the Covid-19 Pandemic using the Cellular Automata Approach and the Resulting Mean Field System: A Case study in Mauritius. *Applied Mathematical Modelling, 111*, 567–589. https://doi.org/10.1016/j.apm.2022.07.008

Ryan, S. J., Lippi, C. A., Boersch-Supan, P. H., Heydari, N., Silva, M., Adrian, J., Noblecilla, L. F., Ayala, E. B., Encalada, M. D., & Larsen, D. A. (2017). Quantifying seasonal and diel variation in Anopheline and Culex human biting rates in Southern Ecuador. *Malaria Journal, 16*(1), 1–10.

Sauer, J. R., Link, W. A., & Hines, J. E. (2020). The North American Breeding Bird Survey, Analysis Results 1966 - 2019: U.S. Geological Survey data release. https://www.sciencebase.gov/catalog/item/5f1836a482cef313ed843104. (Accessed 25 May 2023).

Shaman, J. (2007). Amplification due to spatial clustering in an individual-based model of mosquito–avian arbovirus transmission. *Transactions of The Royal Society of Tropical Medicine and Hygiene, 101*(5), 469–483. https://doi.org/10.1016/j.trstmh.2006.11.007

Sipper, M. (1994). *Non-uniform cellular automata: Evolution in rule space and formation of complex structures. Artificial life IV.*

Sirakoulis, G. C., Karafyllidis, I., & Thanailakis, A. (2000). A cellular automaton model for the effects of population movement and vaccination on epidemic propagation. *Ecological Modelling, 133*(3), 209–223.

Slimi, R., El Yacoubi, S., Dumonteil, E., & Gourbière, S. (2009). A cellular automata model for Chagas disease. *Applied Mathematical Modelling, 33*(2), 1072–1085. https://doi.org/10.1016/j.apm.2007.12.028

StatCan. (2016). *Statistics Canada. Boundary files, 2016 census. Statistics Canada catalogue no. 92-160-X, 2016.*

StatCan. (2022a). Statistics Canada. Table 13-10-0418-01 Crude birth rate, age-specific fertility rates and total fertility rate (live births). https://www150.statcan.gc.ca/t1/tbl1/en/tv.action?pid=1310041801&pickMembers%5B0%5D=1.7&cubeTimeFrame.startYear=2017&cubeTimeFrame.endYear=2021&referencePeriods=20170101%2C20210101&request_locale=en. (Accessed 16 February 2023).

StatCan. (2022b). Statistics Canada. Table 13-10-0710-01 Mortality rates, by age group. https://www150.statcan.gc.ca/t1/tbl1/en/tv.action?pid=1310071001&pickMembers%5B0%5D=1.7&pickMembers%5B1%5D=3.1&cubeTimeFrame.startYear=2016&cubeTimeFrame.endYear=2020&referencePeriods=20160101%2C20200101&request_locale=en. (Accessed 16 February 2023).

StatCan. (2023). *Statistics Canada. 2023. (table). Census profile. 2021 census of population. Statistics Canada catalogue no. 98-316-X2021001. Ottawa* https://www12.statcan.gc.ca/census-recensement/2021/dp-pd/prof/index.cfm?Lang=E. (Accessed 3 April 2023).

Sullivan, B. L., Aycrigg, J. L., Barry, J. H., Bonney, R. E., Bruns, N., Cooper, C. B., Damoulas, T., Dhondt, A. A., Dietterich, T., Farnsworth, A., Fink, D., Fitzpatrick, J. W., Fredericks, T., Gerbracht, J., Gomes, C., Hochachka, W. M., Iliff, M. J., Lagoze, C., La Sorte, F. A., & Kelling, S. (2014). The eBird enterprise: An integrated approach to development and application of citizen science. *Biological Conservation, 169*, 31–40. https://doi.org/10.1016/j.biocon.2013.11.003

Taieb, L., Ludwig, A., Ogden, N. H., Lindsay, R. L., Iranpour, M., Gagnon, C. A., & Bicout, D. J. (2020). Bird species involved in west Nile virus epidemiological cycle in Southern Québec [Article]. *International Journal of Environmental Research and Public Health, 17*(12), 1–19. https://doi.org/10.3390/ijerph17124517. Article 4517.

Talbot, B., Ardis, M., & Kulkarni, M. A. (2019). Influence of demography, land use, and urban form on West Nile virus risk and human West Nile virus incidence in Ottawa, Canada. *Vector Borne and Zoonotic Diseases, 19*(7), 533–539.

Therrien, C., Fournier, É., Ludwig, A., Ménard, J., Charest, H., & Martineau, C. (2019). Phylogenetic analysis of West Nile virus in Quebec, Canada, 2004–2016: Co-circulation of distinct variants harbouring conserved amino acid motifs in North America. *Virology, 537*, 65–73. https://doi.org/10.1016/j.virol.2019.08.019

Todoric D. V. L., Mitri, M. E., Gasmi, S., Stewart, A., Connors, S., Zheng, H., Bourgeois, A.-C., Drebot, M., Paré, J., Zimmer, M., & Buck, P. (2022). *An overview of the national West Nile virus surveillance system in Canada: A one health approach* (Vol. 48, pp. 181–187). https://doi.org/10.14745/ccdr.v48i05a01j, 5.

VanDalen, K. K., Hall, J. S., Clark, L., McLean, R. G., & Smeraski, C. (2013). West Nile virus infection in American robins: new insights on dose response. *PLoS One, 8*(7), Article e68537.

Vanderhoff, N., Pyle, P., Patten, M. A., Sallabanks, R., & James, F. C. American robin (Turdus migratorius), version 1.0.

Vanderhoff, N., Pyle, P., Patten, M. A., Sallabanks, R., & James, F. C. (2016). *American Robin (Turdus migratorius), version 2.0.* Ithaca, NY: Birds of North America. Cornell Lab of Ornithology.

Vichniac, G. (1984). In D. Farmer, T. Toffoli, & S. Wolfram (Eds.), *Simulating physics with cellular automata, inProceedings of an Interdisciplinary Workshop.* North-Holland Physics Publishing.

Vogels, C. B. F., Hartemink, N., & Koenraadt, C. J. M. (2017). Modelling West Nile virus transmission risk in Europe: effect of temperature and mosquito biotypes on the basic reproduction number. *Scientific Reports, 7*(1), 5022. https://doi.org/10.1038/s41598-017-05185-4

Wang, J., Lv, W., Jiang, Y., & Huang, G. (2023). A cellular automata approach for modelling pedestrian-vehicle mixed traffic flow in urban city [Article]. *Applied Mathematical Modelling, 115*, 1–33. https://doi.org/10.1016/j.apm.2022.10.033

Weatherhead, P. J., & McRae, S. B. (1990). Brood care in American robins: Implications for mixed reproductive strategies by females. *Animal Behaviour, 39*(6), 1179–1188. https://doi.org/10.1016/S0003-3472(05)80790-0

White, S. H., del Rey, A. M., & Sánchez, G. R. (2007). Modeling epidemics using cellular automata [Article]. *Applied Mathematics and Computation, 186*(1), 193–202. https://doi.org/10.1016/j.amc.2006.06.126

WHO. (2017). *Global vector control response 2017-2030. Special programme for research training in tropical, diseases*. World Health Organization. https://apps.who.int/iris/handle/10665/259205

Wonham, M. J., De-Camino-Beck, T., & Lewis, M. A. (2004). An epidemiological model for West Nile virus: Invasion analysis and control applications. *Proceedings of the Royal Society B: Biological Sciences, 271*(1538), 501–507. https://doi.org/10.1098/rspb.2003.2608

Young, H. F. (1950). *Territorial behavior in the eastern robin*. University of Wisconsin–Madison.

Zhang, J. P., Jin, Z., & Zhu, H. P. (2018). Birds Movement Impact on the Transmission of West Nile Virus between Patches. *Journal of Applied Analysis and Computation, 8*(2), 443–456. https://doi.org/10.11948/2018.443